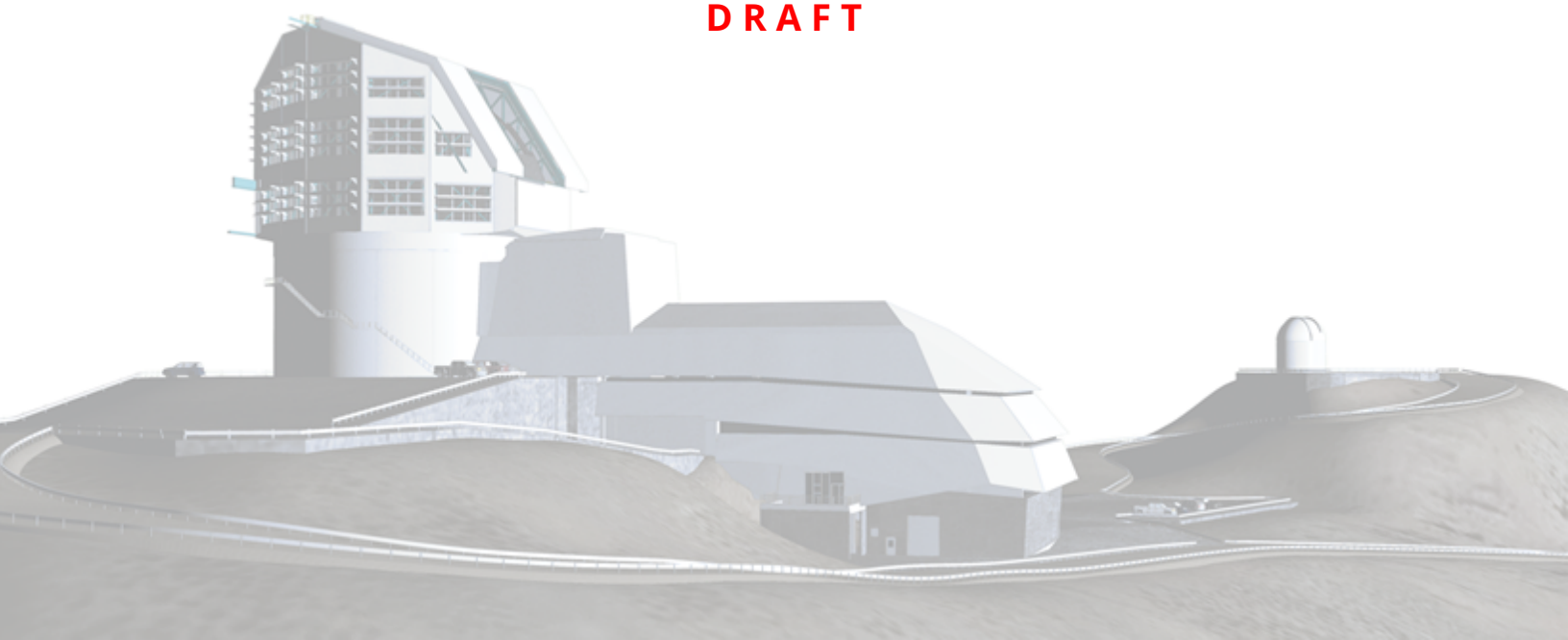

Vera C. Rubin Observatory
Systems Engineering

An Interim Report on the ComCam On-Sky Campaign

Many authors

SITCOMTN-149

Latest Revision: 2024-11-25

DRAFT

Abstract

A summary of what we have learned from the initial period of ComCam observing

Change Record

Version	Date	Description	Owner name
1	YYYY-MM-DD	Unreleased.	Robert Lupton

Document source location: `https://github.com/lsst-sitcom/sitcomtn-149`

Contents

1 Introduction **1**

1.1 Charge 1

2 System Performance Analysis **3**

3 Active Optics System Commissioning **3**

4 Image Quality **3**

5 Data Production **3**

6 Calibration Data **3**

7 Science Pipelines Commissioning Observations **3**

8 Throughput for Focused Light **3**

9 Delivered Image Quality and PSF **3**

10 Instrument Signature Removal **3**

10.1 Phosphorescence 4

10.2 Vampire pixels 4

10.3 Saturated star effects 7

10.4 Gain ratios 7

10.5 Crosstalk 10

10.6 Twilight flats 10

10.7 Operations 13

11 Low Surface Brightness **13**

12 Astrometric Calibration **13**

13 Photometric Calibration **13**

14 Survey Performance **13**

15 Sample Production **13**

16 Difference Image Analysis: Transience and Variable Objects **13**

17 Difference Image Analysis: Solar System Objects **13**

18 Galaxy Photometry **13**

18.1 Comparison to External Imaging 14

18.2 Comparison to External Catalogs 14

18.3 Additional Investigations 18

18.4 Conclusions 18

19 Weak Lensing Shear **18**

20 Crowded Stellar Fields **18**

21 Image Inspection **19**

A References **19**

B Acronyms **19**

An Interim Report on the ComCam On-Sky Campaign

1 Introduction

The Vera C. Rubin Observatory on-sky commissioning campaign using the Commissioning Camera (ComCam) began on 24 October 2024 and is forecasted to continue through mid-December 2024. This interim report provides a concise summary of our understanding of the integrated system performance based tests and analyses conducted during the first weeks of the ComCam on-sky campaign. The emphasis is distilling and communicating what we have learned about the system. The report is organized into sections to describe major activities during the campaign, as well as multiple aspects of the demonstrated system and science performance.

Warning: Preliminary Results

All of the results presented here are to be understood as work in progress using engineering data. It is expected at this stage, in the middle of on-sky commissioning, that much of the discussion will concern open questions, issues, and anomalies that are actively being worked by the team. Additional documentation will be provided as our understanding of the demonstrated performance of the as-built system progresses.

1.1 Charge

We identify the following high-level goals for the interim report:

- **Rehearse workflows for collaboratively developing documentation** to describe our current understanding of the integrated system performance, e.g., to support the development of planned Construction Papers and release documentation to support the Early Science Program [RTN-011]. This report represents an opportunity to collectively exercise the practical aspects of developing documentation in compliance with the policies and guidelines for information sharing during commissioning [SITCOMTN-076].
- **Synthesize the new knowledge** gained from the ComCam on-sky commissioning cam-

paign to inform the optimization of activities between the conclusion of the ComCam campaign and the start of the on-sky campaign with the LSST Camera (LSSTCam).

- **Inform the Rubin Science Community** on the progress of the on-sky commissioning campaign using ComCam.

Other planned systems engineering activities will specifically address system-level verification ([LSE-29] and [LSE-30]) using tests and analysis from the ComCam campaign. While the analyses in this report will likely overlap with the generation of verification artifacts for systems engineering, and system-level requirement specifications will serve as key performance benchmarks for interpreting the progress to date, formal acceptance testing is not an explicit goal of this report.

The groups within the Rubin Observatory project working on each of the activities and performance analyses are charged with contributing to the relevant sections of the report. The anticipated level of detail for the sections ranges from a paragraph up to a page or two of text, depending on the current state of understanding, with **quantitative performance** expressed as summary statistics, tables, and/or figures. The objective for this document is to **summarize the state of knowledge of the system**, rather than how we got there or "lessons learned". The sections refer to additional supporting documentation, e.g., analysis notebooks, other technotes with further detail, as needed. Given the timelines for commissioning various aspects of the system, it is natural that some sections will have more detail than others.

The anticipated milestones for developing this interim report are as follows:

- 18 Nov 2024: Define charge
- 4 Dec 2024: First drafts of report sections made available for internal review
- 11 Dec 2024: Revised drafts of report sections made available for internal review; editing for consistency and coherency throughout the report
- 18 Dec 2024: Initial version of report is released

Warning: On-sky Pixel Image Embargo

All pixel images and representations of pixel images of any size field of view, including individual visit images, coadd images, and difference images based on ComCam commissioning on-sky observations must be kept internal to the Rubin Observatory Project team, and in particular, cannot be included in this report. Embargoed pixel images can only be referenced as authenticated links. See [SITCOMTN-076] for details.

2 System Performance Analysis

3 Active Optics System Commissioning

4 Image Quality

5 Data Production

6 Calibration Data

7 Science Pipelines Commissioning Observations

8 Throughput for Focused Light

9 Delivered Image Quality and PSF

10 Instrument Signature Removal

The quality of the instrument signal removal (ISR) has improved during commissioning, as we create and deploy updated calibration products that better represent the LSSTComCam system. The following discussion summarizes our current understanding of a variety of features,

both expected and newly seen on LSSTComCam, and presents our expected prognosis of the behavior of the full LSSTCam.

10.1 Phosphorescence

There are regions on some of the detectors (most visible in R22_S01, detector=1) which show bright emission, particularly at bluer wavelengths, as shown in Figure 1. This is believed to be caused by a thin layer of remnant photo-resist from the manufacturing process that remained on the detector surface, and is now permanent due to the subsequent addition of the anti-reflective coating. In addition to the large areas, there are also discrete point-source-like or cosmic-ray-like defects caused by accumulations of this material. Adding to the difficulty of mitigating these defects is that this photo-resist is known to be phosphorescent, explaining why these regions are more noticeable in the bluer filters.

The initial studies of this show that these features can continue to emit light up to several minutes after they've been illuminated. Due to the long duration of these features, we decided to place manual defect masks over the worst regions. The first of these manual masks takes up about 3.5% of that detector, smaller than but consistent with estimates that this would create a pixel loss of approximately one amplifier.

The ITL detectors in LSSTCam are believed to have been cleaned better, so this should be less of an issue on the full camera.

10.2 Vampire pixels

There are defects on LSSTComCam that have been classified as "vampire" pixels, as they appear as a bright defect with a (generally) axisymmetric region surrounding the bright core, as if the defect is draining charge from its neighbors. The naming is at least broadly correct, as integrating to large radii shows that these regions do appear to conserve charge. There is an intensity dependence that makes these vampire pixels different than standard hot pixels, as these pixels do not show up on dark frames, only on flats and science exposures, where the detector surface is illuminated. After the initial discovery of the bright obvious vampires, we added new masking code that identifies the bright cores that are above 2.0 on the combined flat (pixels that are greater than 200% of the median flat level), and adds circular masks to the defect list. This appears to find the most problematic examples, but as we have improved

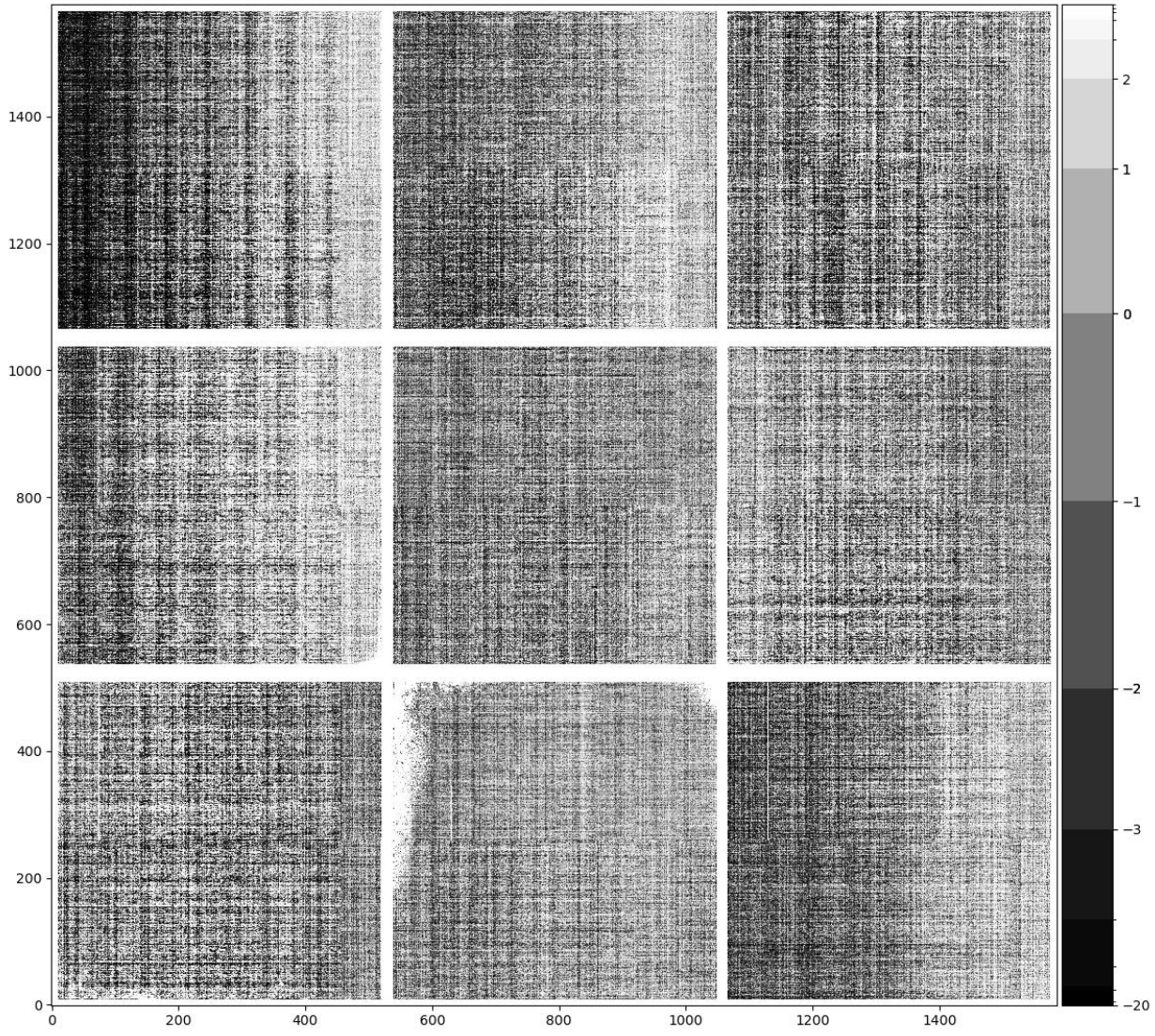

FIGURE 1: The phosphorescence seen in R22_S01, shown here in a dark exposure taken after a series of twilight flats (exposure=2024112000065). This material absorbs light at bluer wavelengths and re-emits that energy over a wide range of wavelengths.

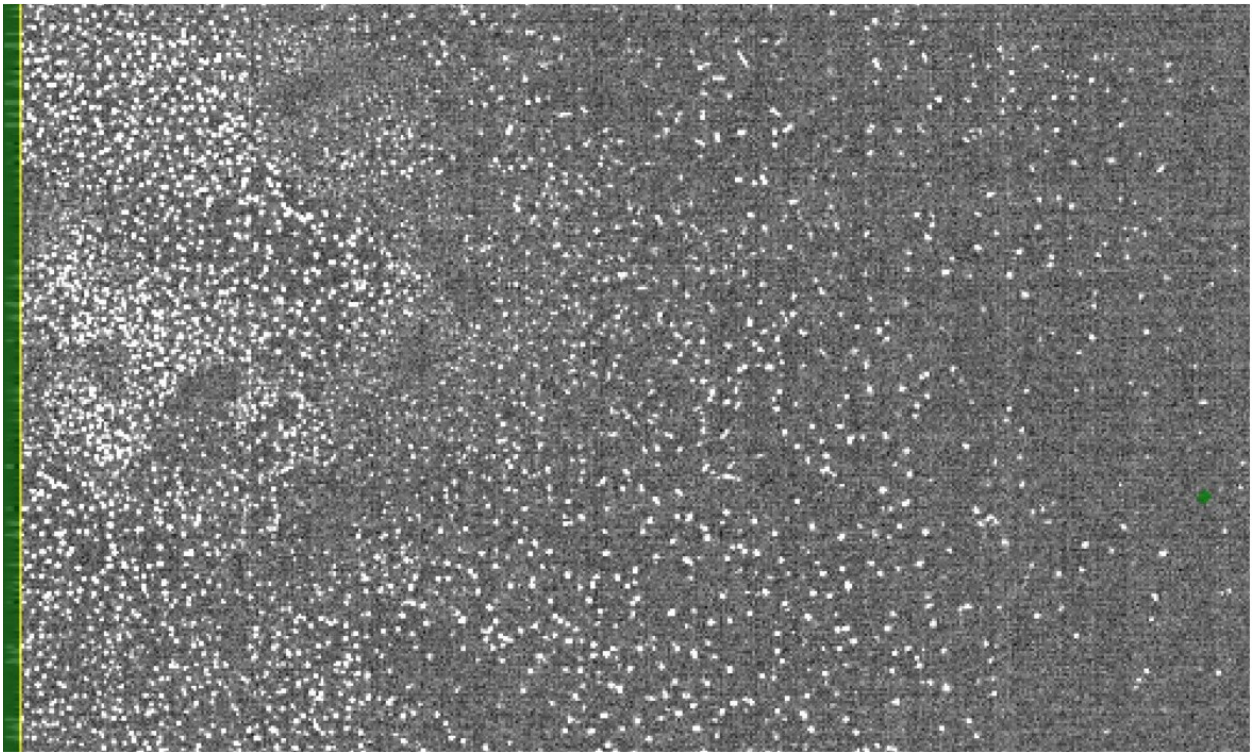

FIGURE 2: A full-resolution view of the edge of R22_S01. The features shown in this image are point-like sources caused by the trapped phosphorescence photo-resist.

flat quality during commissioning, we are finding that there is a sub-population that are not as severe, but likely have a similar physical mechanism. This population is still bright on the flat, with peaks around 1.2 (20% elevated relative to the flat), and may need to be masked as well. From an initial study in the lab, it appears that all ITL detectors on LSSTCam have a few of these kinds of defects, with two detectors approaching similar contamination levels as R22_S10 on LSSTComCam.

10.3 Saturated star effects

Although we expected to find saturated star trails coming from bright sources, the observed behavior of these trails is unique. Saturation spikes on most cameras appear as streaks extending from the core of the bright source along the direction of the parallel transfers, and truncate as the charge bleeds run out of charge (and can no longer overcome the potentials defining the pixel). The trails seem with LSSTComCam, however, extend the entire height of the detectors, crossing the midline break. These trails are also not at the expected high state, with the centers of these trails having flux levels lower than the average sky levels, creating dark trails. On the worst saturated objects, there is also evidence of charge pile-up near the serial readout, which can then create fan-like bright features at the edge of the detector. Those bright features can also then crosstalk onto other amplifiers.

The underlying physics is not well understood, and further study will be needed to see if we can correct these trails outside of the regions of charge buildup. Until we have a correction, we plan to begin masking both the trail and the fan-spread near the serial register.

Although we haven't seen identical features on LATISS, the presence of these odd trails on all LSSTComCam detectors suggests that this is a property of the ITL devices, and so will likely be seen on LSSTCam as well.

10.4 Gain ratios

LSSTComCam has been the first large-scale application of the updated "IsrTaskLSST" task, which uses a model of how the various signals combine to form the raw images to inform how we correct those signals during the ISR process. One improvement of this new task is that we now apply per-amplifier gains before flat correction, removing the gain component that was previously included in the flat correction. This results in the flat containing mainly

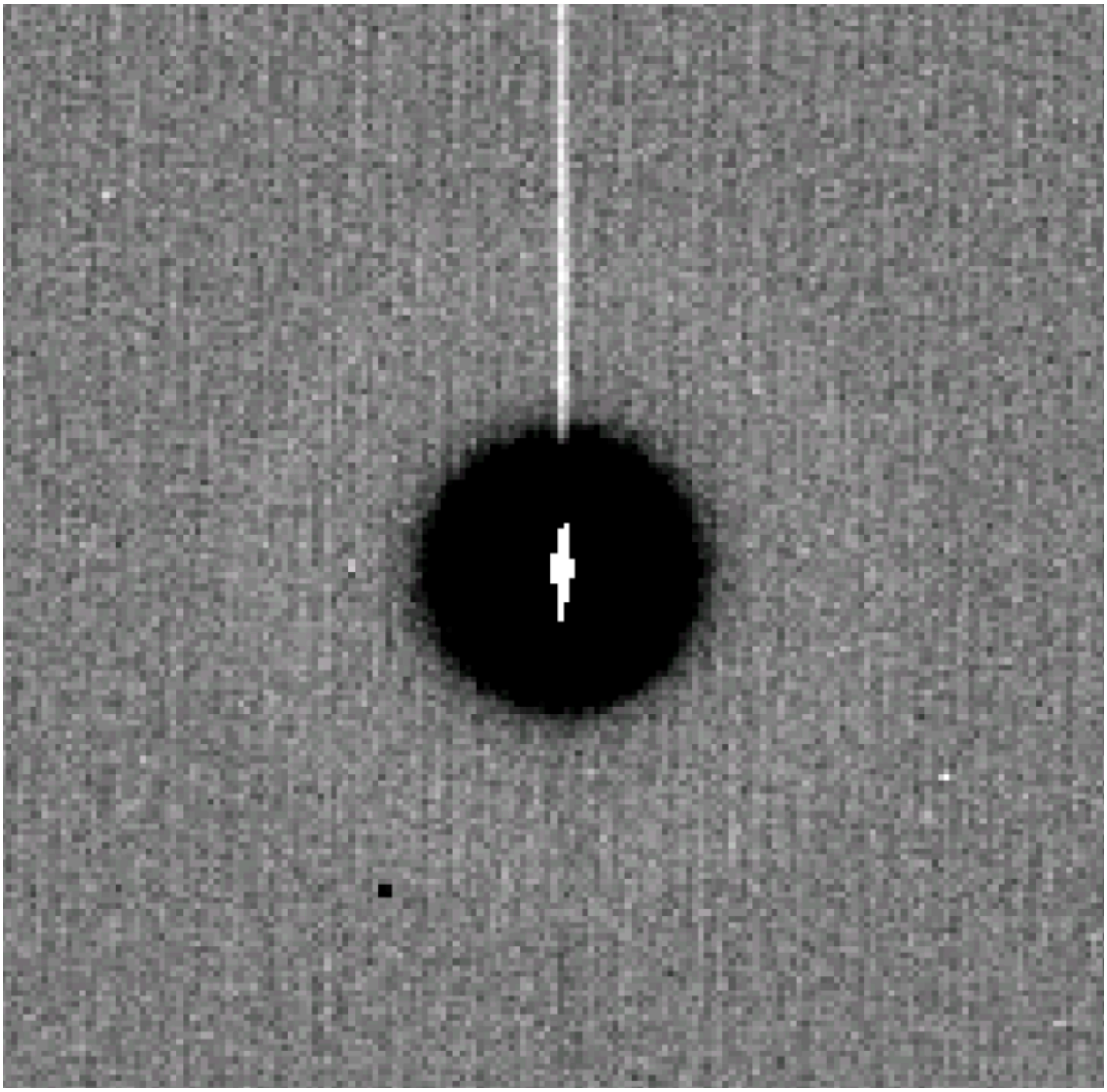

FIGURE 3: A close up of one of the largest vampire pixels. The bright core and region of depletion are clearly visible. Currently we only mask the core and depleted region, but will be extending this to mask the persistence-like trail that this feature leaves in the next few weeks.

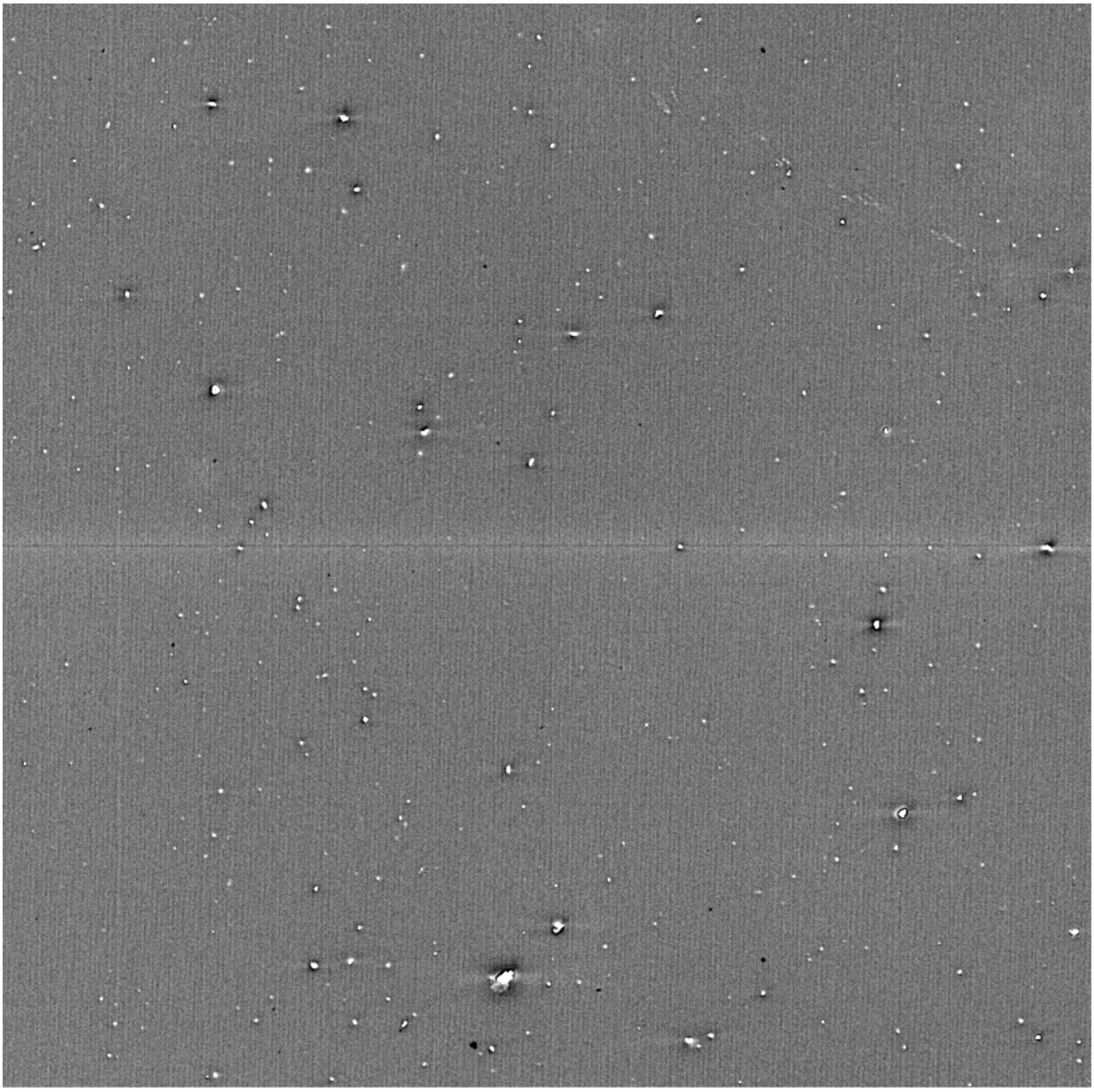

FIGURE 4: A view of detector R22_S10 in y-band, which has a large number of less significant vampire pixels.

QE and illumination patterns, which is much "flatter" than flats that also include gain terms (which offset the amplifiers relative to each other).

If we have properly diagonalized the flats and the gains, we would expect that applying the gain correction would create images with consistent sky levels across different amplifiers. However, when we look at images taken on-sky, our initial gain values result in some amplifiers being significantly different than their neighbors. The gains that we use are derived from the photon transfer curve (PTC), which uses flat pairs at different flux levels to monitor the properties of the noise. We have two of these sequences taken in the lab, and they disagree at the few percent level. This is similar in scale to the errors necessary to explain the on-sky differences. Further complicating this issue, the offsets seen in twilight data (used for flats) and that seen during the night also seem to differ. These differences so far have not been found to correlate with any device temperature, time, or voltage values. The gain correction fix appears to be stable, as we've only needed to generate and apply it once.

10.5 Crosstalk

We are currently using crosstalk values that were constructed by averaging the lab-based ITL measurements taken on LSSTCam. These are working better than expected, with residuals post correction being only a few electrons peak to peak. We plan to do a more complete crosstalk study using on-sky data, but the current results suggest that these lab measurements are sufficient for LSSTComCam, and expect the same to be true for LSSTCam.

10.6 Twilight flats

There is no flat screen currently available for the main telescope, and so we have constructed twilight flats for all bands using exposures taken to have median counts between 15000-20000 ADU. We have some dithering in the inputs, which have allowed us to reduce the impact of stars that print through into the flat. This reduction of non-sky signals is imperfect, and the current i-band flat shows a satellite trail as a result We are working to replace this flat using newly taken data.

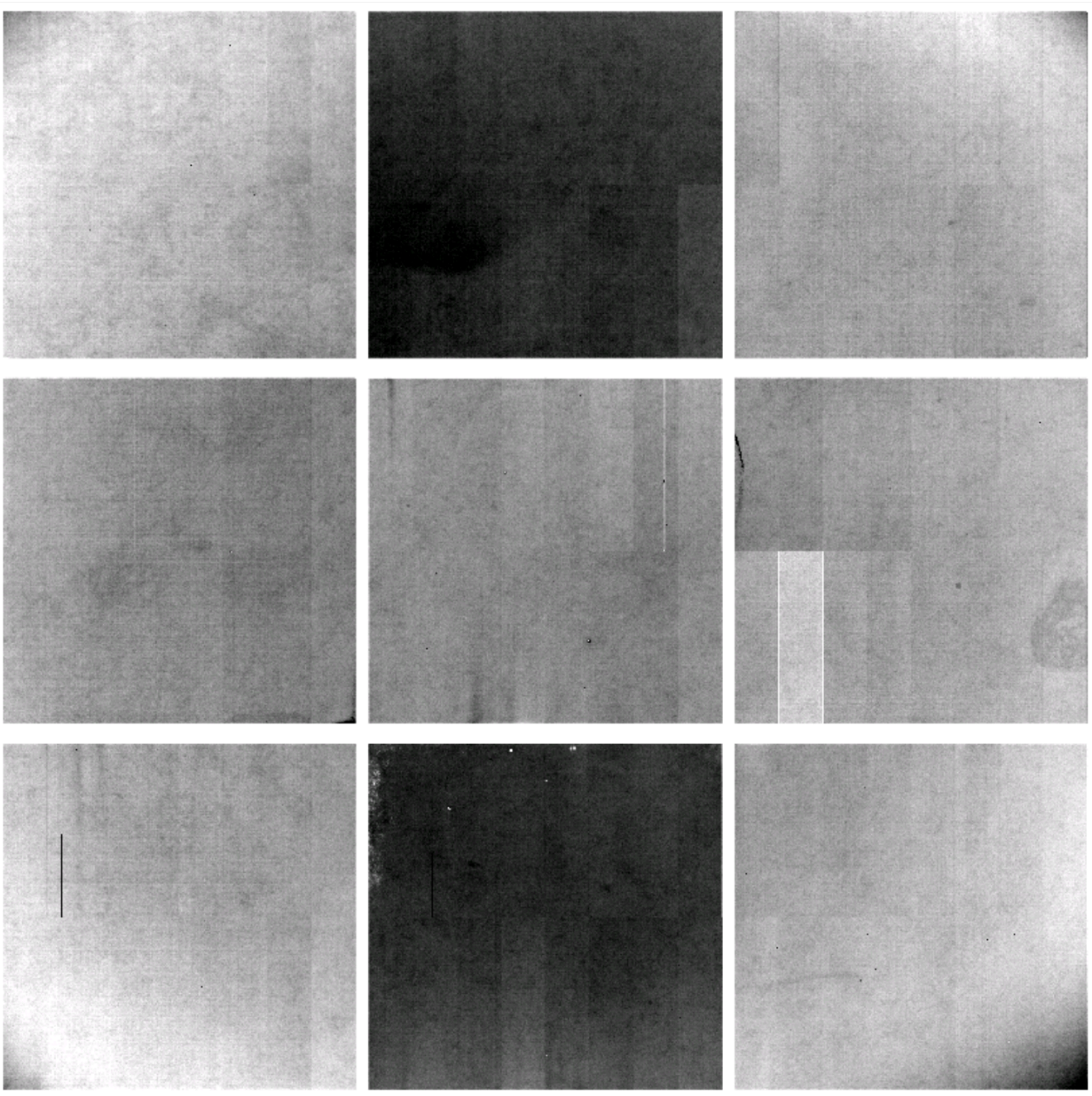

FIGURE 5: The ratio of the twilight-flat divided by a flat constructed from 94 r-band science frames. The scaling ranges from 0.9905 to 1.007. The visibility of amplifiers is caused by the unknown gain errors. The bottom right corner amplifier (C07) on R22_S21 is one of the indicator amplifiers, as it diverges from its neighbors. Although the C00-C03 amplifiers in R22_S12 also show significant offsets, these amplifiers also have an unrelated CTI issue, making them less reliable indicators.

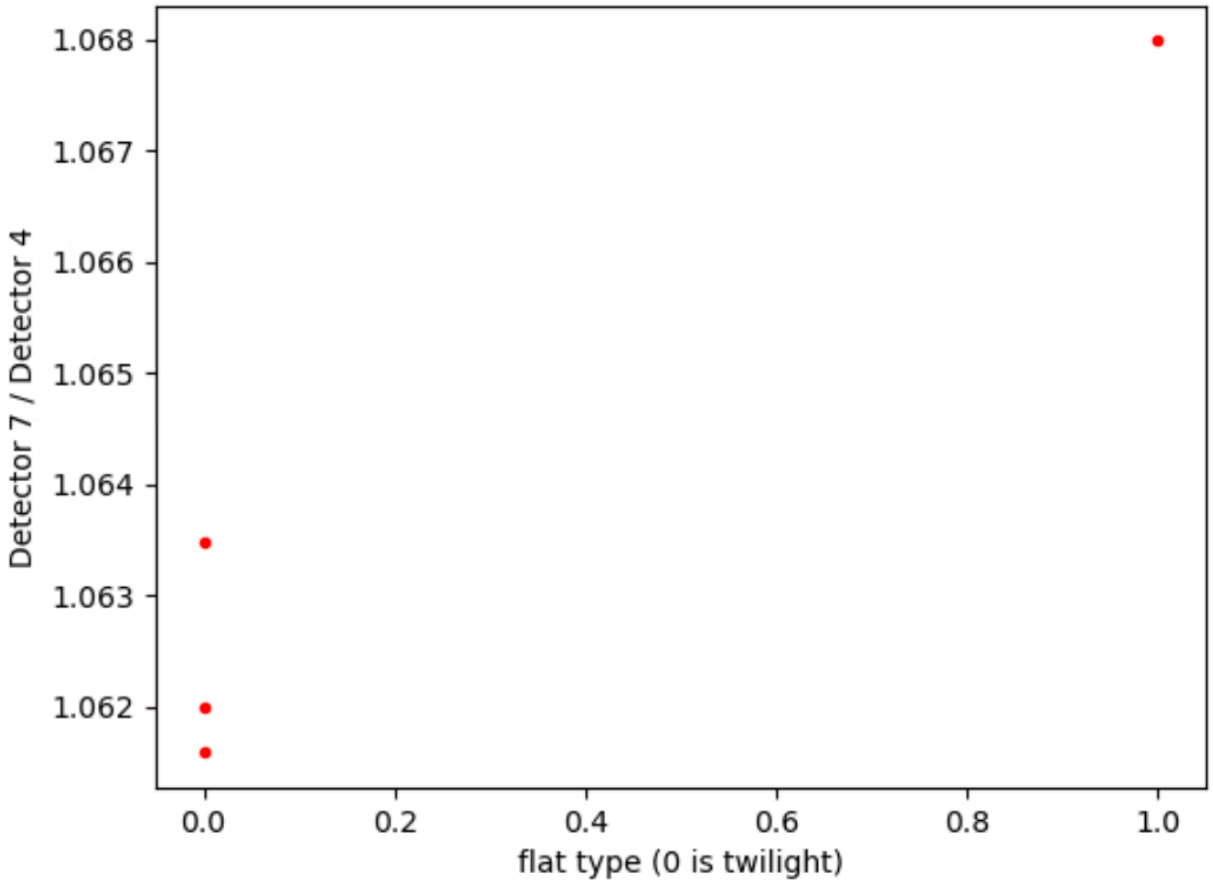

FIGURE 6: A comparison of the gain ratio between amplifiers in R22_S12. C07 is chosen as the indicator amplifier, and C04 is the reference. We have three twilight flat measurements taken at different rotator angles, and one from the 94 input sky flat.

10.7 Operations

The Telescope and Auxiliary Instrumentation Calibration Acceptance Board (TAXICAB) has been meeting previously to discuss LATISS calibrations, and has been helping manage calibrations for LSSTComCam. This process has not prevented problematic calibrations from being deployed (like the i-band flat with the satellite trail), but it has ensured that multiple people have checked some set of results. We are generating calibration verification reports regularly as part of this process (available at `https://s3df.slac.stanford.edu/people/czw/cpv_reports/`), and plan to add new metrics and checks to these as we discover more features of these detectors.

11 Low Surface Brightness

12 Astrometric Calibration

13 Photometric Calibration

14 Survey Performance

15 Sample Production

16 Difference Image Analysis: Transience and Variable Objects

17 Difference Image Analysis: Solar System Objects

18 Galaxy Photometry

Galaxy photometry investigations so far have used the Extended Chandra Deep Field-South (ECDFS) due to the availability of public external reference data, including space-based imaging from the Hubble Space Telescope (HST). Broadly, we have done (or soon will be doing) comparisons to matches against external catalogs and from synthetic source injection (SSI) in

coadds. Some preliminary investigations were done with visual inspection of external images.

18.1 Comparison to External Imaging

We downloaded a subset of the Hubble Legacy Fields (HLF, https://archive.stsci.edu/prepds/hlf/) imaging for the GOODS-South field, which included programs covering the original Chandra Deep Field-South and parallel fields now part of ECDFS. Significantly overlapping coverage is available in F435W, F606W, F775W and F814W, as well as four redder bands. F775W is of particular interest for galaxy photometry since it was designed to match the SDSS i-band filter.

Visual inspection of a particular group of photogenic galaxies in the HST imaging revealed an excess point source in the ComCam imaging from Nov. 8, which was subsequently found to match the position of an alert issued by several ZTF brokers in early September. We experimented with using the HST image as a template for difference imaging by PSF matching and resampling to ComCam resolution. This can be done relatively successfully on a per-object basis, but unfortunately, the image registration/warping for the HST images is too inconsistent to make it worthwhile on patch scales without re-warping one image or the other.

Besides visual inspection, no other uses of or comparisons to external imaging have yet been demonstrated. DM-47576 (https://rubinobs.atlassian.net/browse/DM-47576) has been informally assigned to an in-kind contributor to make loading and displaying HST images more convenient should a need arise.

Joint modelling of space and ground imaging has been demonstrated with MultiProFit in COSMOS with the Subaru Hyper Suprime-Cam (HSC) and HST data on DM-46497 (https://rubinobs.atlassian.net/browse/DM-46497) but has not been attempted with ComCam data and is not considered a high priority, in part due to the aforementioned astrometry/warping issues.

18.2 Comparison to External Catalogs

DM-47234 (https://rubinobs.atlassian.net/browse/DM-47234) compared the tract 5063 20241120 DRP object table galaxy photometry with the latest HLF and Dark Energy Camera Legacy Survey DECaLS (DECaLS, https://www.legacysurvey.org/decamls/) catalogs.

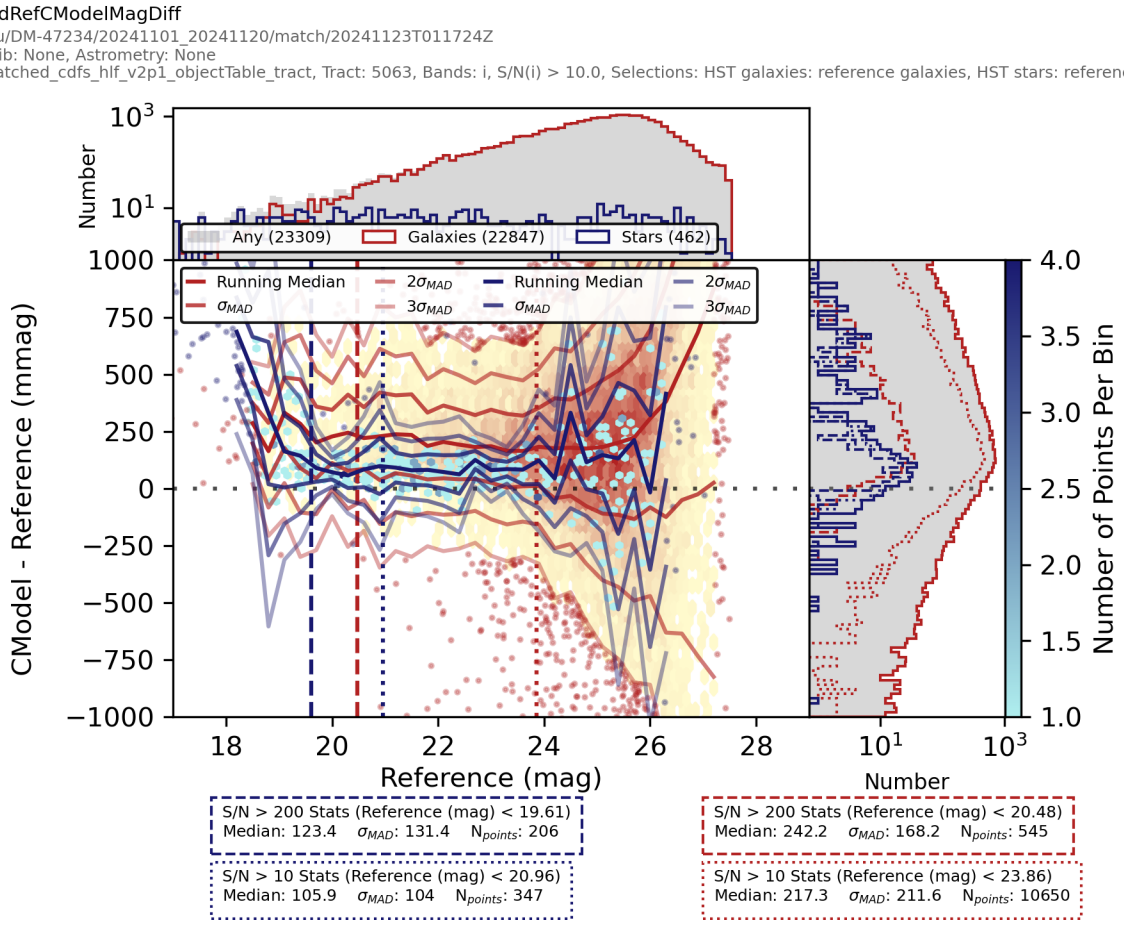

FIGURE 7: Difference between i-band CModel magnitudes and HST F775W magnitudes in ECDFS.

Figure 18.2 shows difference between i-band CModel magnitudes and the HLF HST F775W SourceExtractor magnitudes for both stars and galaxies, using the HST star-galaxy classification. The median difference in both stellar and galaxy photometry is fairly flat across 19<i<25, but also quite large at about 175 mmag for galaxies and 75 mmag for stars. Presuming that the difference in stellar photometry is mainly a calibration issue, the differential between galaxies and stars is still more than a factor of 2 (and still more in quadrature). This could be due to differences in methodology; the HST SourceExtractor-derived magnitudes are more like aperture photometry than a model fit.

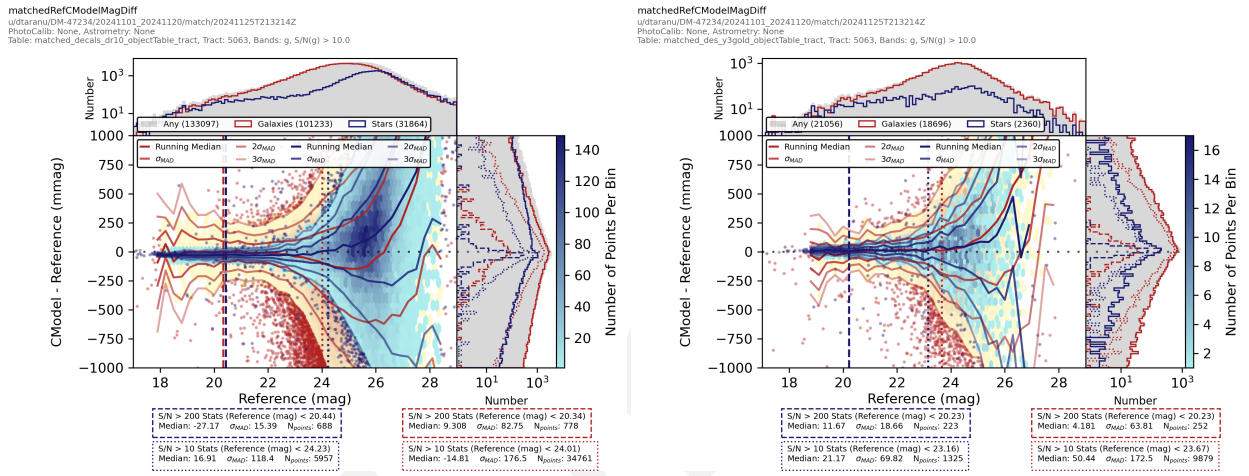

FIGURE 8: Difference between g-band CModel magnitudes and DECaLS/DES-Y3G catalog values in ECDFS.

Figure 18.2 shows the difference between g-band CModel magnitudes and measurements from two Dark Energy Survey (DES) DECam (Dark Energy Camera)-based catalogs. The DECaLS (Dark Energy Camera Legacy Survey) DR10 processing is more recent and includes model photometry, selecting the least complicated model required to provide a good fit from a PSF to a single free Sersic fit. The Dark Energy Survey Year 3 Gold (DES-Y3G) sample is an older, shallower dataset, albeit using pipelines more similar to the ComCam/DRP pipelines. The median difference between stellar magnitudes is relatively small but varies with magnitude and between the two catalogs. However, given the difference between filters and that no color term corrections have been applied, both the medians offset and scatter of 10 to 30 mmag are acceptable. Bright ($g < 20.3$) galaxies have median offsets smaller than 10 mmag and scatter of 82 and 64 mmag in DECaLS and DES-Y3G, respectively.

Figure 18.2 shows r-band magnitude difference plots. Here, the median difference for stars are magnitude-dependent in both catalogs, suggesting that color terms are more important. Similarly, the scatter is much larger, at about 80mmag for $r < 20$. However, the magnitude

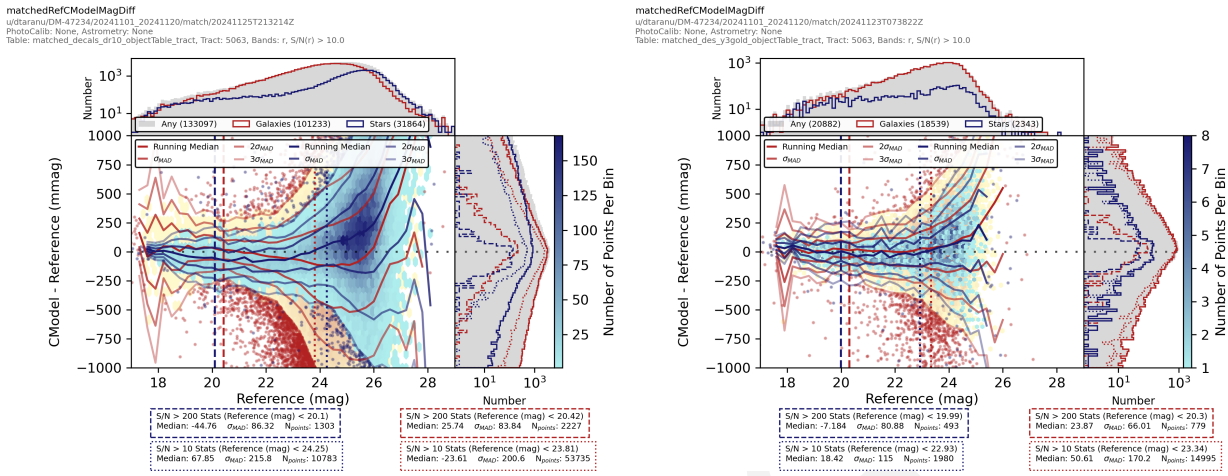

FIGURE 9: Difference between r-band CModel magnitudes and DECaLS/DES-Y3G catalog values in ECDFS.

dependence in the median difference is stronger in DECaLS, both for stars and galaxies. Inspection of the $g-r$ versus $r-i$ stellar locus plot (not shown) reveals that DECaLS photometry has a substantial fraction (about 10%) of outliers, some even a full magnitude off the stellar locus. At any rate, the scatter in galaxy magnitudes is not much larger than that for stars (in fact, it is noticeably smaller in DES-Y3G). Additionally, in DES-Y3G, the median magnitude difference is fairly flat for $19 < r < 23$, so despite the numerous differences in hardware and software, the two catalogs are not inconsistent. The i-band photometry in DECaLS shows qualitatively similar but quantitatively worse pathologies and is omitted for brevity.

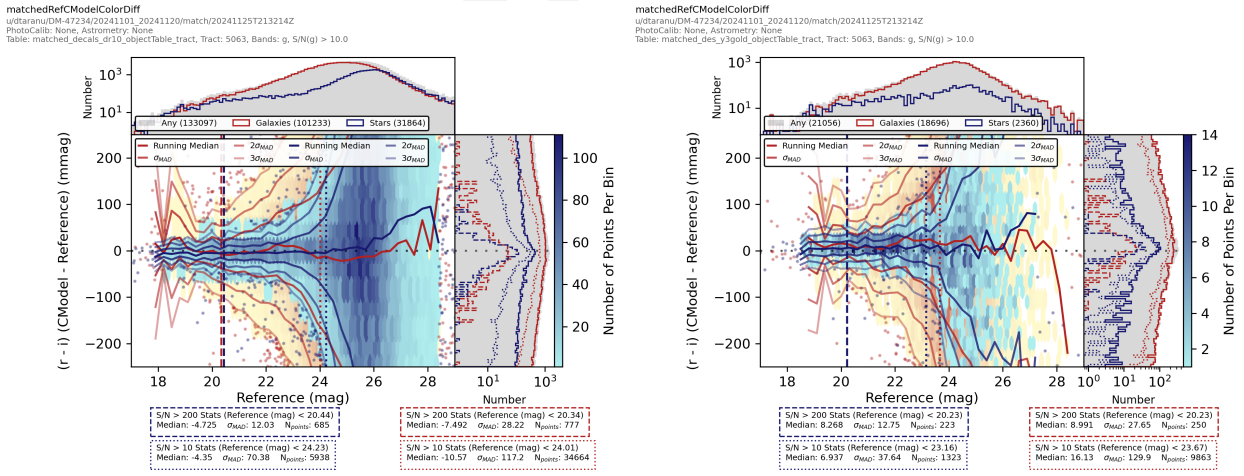

FIGURE 10: Difference between $r-i$ CModel colors and DECaLS/DES-Y3G catalog values in ECDFS.

The $r-i$ color differences shown in Figure 18.2 are similar between all three catalogs. The

median differences are very small, albeit different in sign between the two pairs of catalogs. The scatter in star color differences is nearly constant to about 22nd magnitude, whereas for galaxies it scales with signal-to-noise to a minimum of about 25mmag at 20th mag (photometry for brighter galaxies is limited by model inadequacy and irregular structure). In short, galaxy colors appear quite consistent between all three catalogs, although how the small differences impact derived quantities like photometric redshifts remains to be seen.

18.3 Additional Investigations

Analysis of the accuracy of magnitude and color errors await the implementation of synthetic galaxy injection in DM-47185 (`https://rubinobs.atlassian.net/browse/DM-47185`). Some analysis is possible with matching to reference catalogs; however, besides the problems with the DECaLS photometry, we are not yet taking into account reported errors on reference fluxes (which may themselves be underestimated).

Besides single-band/forced CModel photometry, MultiProFit multi-band (gri) single Sersic fits have been run on a single patch in tract 5063 on DM-47526 (`https://rubinobs.atlassian.net/browse/DM-47526`) but have yet to be analyzed. Other algorithms like aperture, GaAP and Kron magnitudes/colors have yet to be compared.

18.4 Conclusions

Galaxy photometry in ECDFS appears consistent with at least two different catalogs covering the same field (one space based) and the differences identified in a third (DECaLS) appear to be peculiar to that catalog, not our own processing. This is not to say that the galaxy photometry is optimal, as hardware and software differences make it difficult to quantify expected differences. Comparisons to external data should be more illuminating once we have coadds in the COSMOS field and can compare to HSC imaging with the same pipeline versions.

19 Weak Lensing Shear

20 Crowded Stellar Fields

21 Image Inspection

A References

[SITCOMTN-076], Bechtol, K., on behalf of the Rubin Observatory Project Science Team, S.R., 2024, Information Sharing during Commissioning, URL https://sitcomtn-076.lsst.io/, Vera C. Rubin Observatory Commissioning Technical Note SITCOMTN-076

[LSE-29], Claver, C.F., The LSST Systems Engineering Integrated Project Team, 2017, LSST System Requirements (LSR), URL https://ls.st/LSE-29, Vera C. Rubin Observatory LSE-29

[LSE-30], Claver, C.F., The LSST Systems Engineering Integrated Project Team, 2018, Observatory System Specifications (OSS), URL https://ls.st/LSE-30, Vera C. Rubin Observatory LSE-30

[RTN-011], Guy, L.P., Bechtol, K., Bellm, E., et al., 2024, Rubin Observatory Plans for an Early Science Program, URL https://rtn-011.lsst.io/, Vera C. Rubin Observatory Technical Note RTN-011

B Acronyms

Acronym	Description
ADU	Analogue-to-Digital Unit
COSMOS	Cosmic Evolution Survey
DECaLS	The Dark Energy Camera Legacy Survey
DECam	Dark Energy Camera
DES	Dark Energy Survey
DM	Data Management
DR10	Data Release 10
DRP	Data Release Production
HSC	Hyper Suprime-Cam
HST	Hubble Space Telescope

ISR	Instrument Signal Removal
ITL	Imaging Technology Laboratory (UA)
LATISS	LSST Atmospheric Transmission Imager and Slitless Spectrograph
LSST	Legacy Survey of Space and Time (formerly Large Synoptic Survey Telescope)
PSF	Point Spread Function
QE	quantum efficiency
RTN	Rubin Technical Note
SDSS	Sloan Digital Sky Survey
SE	System Engineering
SSI	Synthetic Source Injection
ZTF	Zwicky Transient Facility